1991 SCA Conference Paper Number 9111

NUCLEAR MAGNETIC RESONANCE IMAGING OF SODIUM-23 IN CORES

by

P. N. Tutunjian, H. J. Vinegar and J. A. Ferris

Shell Development Co.
Houston, Texas

ABSTRACT

Sodium (^{23}Na) is an NMR-active nucleus with considerable petrophysical importance because sodium is the predominant cation in reservoir brines. This paper presents the first NMR images of ^{23}Na inside cores. Several core applications are demonstrated, including measuring core salinity, 1-D profiling, and 3-D imaging of brine ingress into cores.

INTRODUCTION

Most petrophysical applications of nuclear magnetic resonance (NMR) have used either proton (^{1}H) or carbon (^{13}C) nuclei.[1-5] ^{1}H NMR has been utilized for measuring porosity, oil/water saturations, and permeability,[1-4] and ^{13}C NMR for measuring oil saturation, oil viscosity, and carbonate mineral content.[5,6]

Because sodium is the predominant cation in formation brines, another NMR-active nucleus with considerable petrophysical importance is sodium (^{23}Na). Formation salinity is essential for interpreting resistivity logs, but the salinity may not be known in a new area or in old fields after years of waterflooding. Sodium NMR may then be useful for determining brine salinity inside unflushed cores in cases of unknown formation salinity.

Other applications of sodium NMR include measuring sodium diffusion coefficients in cores, imaging mud filtrate invasion, imaging salinity variations during flooding experiments and checking completeness of salt removal in core extractions. Still other potential applications include nondestructive measurements of cation exchange capacity and sodium transport number for quantifying clay conduction in shaly sands.

SENSITIVITY

The major technical difficulty with obtaining ^{23}Na NMR is its very low sensitivity, about $^{1}/_{10}$ that of the proton. Table 1 compares several nuclei of petrophysical importance, listing their nuclear spin, gyromagnetic ratio (gamma), natural abundance, relative sensitivity (i.e., at constant field for equal number of nuclei) and absolute sensitivity (i.e., product of relative sensitivity and natural abundance). Petrophysical ^{23}Na imaging would appear to be particularly difficult considering sodium's low absolute sensitivity, its dilution in brine (maximum concentration of 5.416 Molar at 25°C), and the further volumetric reduction inside a core due to porosity and oil saturation.

The situation is ameliorated, however, because ^{23}Na has spin 3/2 and a relatively large nuclear quadrupole moment ($+0.14 \times 10^{-24}$ e-cm^2). Quadrupole interactions in the liquid are particularly efficient, and sodium's quadrupolar-enhanced nuclear spin-lattice relaxation facilitates rapid data acquisition and good signal-to-noise spectra. The ^{23}Na spin-lattice relaxation times T_1 can be 1-2 orders of magnitude shorter than those for ^1H so that the lower absolute sensitivity of ^{23}Na is partially offset by the ability to signal average ^{23}Na data at a much faster rate.

APPARATUS

The spectroscopic measurements reported here were made on three NMR spectrometers: General Electric CSI-2T (^1H - 85 MHz, ^{23}Na - 22.6 MHz), Bruker WP-100 MHz (^{23}Na - 28 MHz), and Bruker CXP-200 MHz (^{23}Na - 46 MHz). NMR imaging was performed on the GE CSI-2T using a 3-in. ID sodium spectroscopy/imaging RF coil. The sodium RF imaging coil is of "birdcage" design with high spatial uniformity as described elsewhere and a 50-microsecond recovery time.[3] The gradient coils are self-shielded S-150 inserts which rapidly switch gradients up to 20 Gauss/cm in a 6-in. ID region in less than a few hundred microseconds. The CSI-2T utilizes an Oxford Instruments 31 cm horizontal bore superconducting magnet, whereas the WP-100 and CXP-200 use vertical high resolution superconducting magnets.

SPECTROSCOPIC ^{23}Na MEASUREMENTS

Brine Solutions

Prior to implementing ^{23}Na imaging techniques, simple 90 degree pulse-and-acquire NMR spectra of NaCl brines were obtained using the WP-100 spectrometer. A series of ten brine solutions, ranging from 0 ppm to 200,000 ppm NaCl, were used to verify the linearity of the ^{23}Na NMR response. The NMR acquisition parameters are shown in Table 2.

Figure 1a plots the integral of the ^{23}Na NMR intensity vs sodium chloride concentration, while Figure 1b shows a ten times expanded scale of the low salinity range with the same linear regression fit. These figures show that, in brine solutions, measurement linearity extends from zero salt concentration up to about 100,000 ppm NaCl. The reason for the departure from linearity is radiofrequency (RF) attenuation in the highly conductive brine, which decreases the quality factor Q of the coil and lengthens the 90 degree RF pulse. In cores, RF attenuation should not be a serious factor since the electrical conductivity of the core will be reduced relative to bulk solution by a factor equal to the electrical formation factor (typically 10-100).

Clean Carbonates and Sandstones

A suite of ten samples of Indiana limestone (10 mm OD x 1 in. long, porosity = 13%) plugged from a common block were saturated with the same set of sodium chloride brines from 0 to 200,000 ppm NaCl. Figure 2a shows the 23Na NMR intensity vs sodium chloride concentration is linear over the entire concentration range. Figure 2b is replotted for the low concentration range, which shows the NMR method continues to be linear with the same slope and has adequate signal-to-noise down to the lowest salinities (500 ppm NaCl). Note that the scatter in this data set includes porosity variations between the ten limestone samples.

Table 3 compares NMR and weight measurements of ^{23}Na for a suite of carbonates and clean sandstones saturated with 4.0 M NaCl brine. The average error of estimation is 3.1% with an increasing degree of underestimation with shaliness. These NMR data indicate that sodium concentration can be measured accurately inside clean carbonates and sandstones.

In order to convert sodium concentration into brine salinity, the volume of water in the core must also be determined. This may be measured independently by ^{1}H chemical shift NMR (to distinguish oil from water),[2-4] or alternatively, Dean-Stark extraction can be used to measure the water volume in the core.

Another application of ^{23}Na NMR is checking the completeness of salt removal during core extractions. The brine salinity may be measured during the chloroform/methanol extraction process by obtaining ^{23}Na NMR spectra of the refluxed solvent. The completeness of salt extraction can be monitored by successive NMR measurements on both core and extracted fluid.

Sodium Minerals and Shaly Cores

In order to use sodium NMR for salinity measurements in cores, it is important not to measure contributions from various sodium-containing minerals which could also be present in the rock matrix. This is not a problem for liquid state ^{23}Na NMR because sodium has an electric quadrupole moment so that any surface or bulk interactions which disturb cubic symmetry around the sodium ion broaden the NMR linewidth considerably. A narrowband NMR spectrometer optimized for liquid spectra will therefore not detect sodium-bearing solid minerals.

In order to verify this, a wideband solid state NMR spectrometer (CXP-200) was used to measure the ^{23}Na linewidth for several pure sodium minerals. Figure 3 compares the ^{23}Na spectra of (a) 200,000 ppm NaCl brine in Indiana limestone, (b) crystalline sodium chloride, (c) sodium carbonate, (d) sodium metasilicate, and (e) dry sodium bentonite. The linewidths are tabulated in Table 2, which shows that sodium nuclei in solid sodium-bearing minerals have at least an order of magnitude greater linewidth relative to mobile sodium in the electrolyte. The NMR acquisition parameters can therefore be narrowbanded to reject the contribution from solid sodium minerals.

In shaly sands, however, because sodium clay counterions involved in clay conduction have a mobility of the same order of magnitude as free electrolyte mobility, one would expect the sodium NMR measurement to detect both free electrolyte and clay counterions. Figure 3 also compares the ^{23}Na NMR linewidth of (a) 200,000 ppm NaCl brine in Indiana limestone and (f) Na-bentonite clay hydrated with fresh water. Because of the similar linewidth (see Table 2), liquid state ^{23}Na NMR measurements will include both sodium electrolyte and sodium counterion concentrations.

As previously observed by proton NMR,[4] the spectral linewidth for sodium in shaly sands can be up to fifty times larger than in clean cores. Even though the absolute sodium linewidths are typically $1/4$ those of the proton (due to the inverse dependence of paramagnetic susceptibility-broadening on gyromagnetic ratio), ^{23}Na NMR probes with short dead times are still required for shaly sands. Sodium experiments in shaly sands are in progress, combining the use of solid-state NMR probes having less than 10-microsecond recovery time and spin echo sequences designed to reject signals from solid sodium minerals.

Relaxation Times

Figure 4 plots the ^{23}Na NMR spin-lattice relaxation times (T_1) vs the square root of brine concentration for a suite of brine solutions from 0.005 M to 5 M at 25°C. T_1 was measured on the GE CSI-2T with an inversion recovery pulse sequence $(180\text{-}T\text{-}90)_n$. For comparison, Figure 4 also plots the Na^+ tracer-diffusion coefficient data in NaCl brines at 25°C reported by Wang.[6] As expected, there is an excellent correlation between the ^{23}Na T_1 and the ^{23}Na tracer-diffusion coefficient. This is because, for very short correlation times, T_1 is directly proportional to translational diffusion.[7] In this extreme narrowing condition, for spin 3/2 nuclei relaxing by quadrupole-electric field gradient interactions in a liquid, the spin-lattice relaxation rate (1/T1) is

$$\frac{1}{T_1} = \left(\frac{1}{45}\right)\frac{a^2}{D}\left(1 + \frac{\eta^2}{3}\right)\left(\frac{eQ}{\hbar}\frac{\partial^2 V}{\partial z^2}\right)^2$$

where D is the translational diffusion coefficient, a is the radius of the hydrated sphere for the Na+ ion in Stokes formula, $\left(\frac{eQ}{\hbar}\frac{\partial^2 V}{\partial z^2}\right)$ is the quadrupolar coupling constant where e is the electronic charge, Q is the quadrupole moment, and $\partial V/\partial z$ is the largest value of the field gradient in the molecular frame, and η is the asymmetry parameter of the electric field gradient.

Over this range of concentrations, there is a 39% decrease in T_1 as salinity is increased (from 62 msec to 38 msec) with most of the decrease in T_1 occurring in the high salinity range above 1 M NaCl. NMR linewidth measurements indicate a 24% increase over the same range of NaCl concentrations (from 38 Hz to 47 Hz). The small hump in diffusion coefficient and T_1 in the moderate concentration range from 0.7 M to 1.0 M NaCl is attributed to distortion in the structure of water by the presence of the strongly hydrated sodium ion.[6] The local distortion in water structure causes the tracer-diffusion coefficient of the ion to increase with salt concentration. At high concentrations the increasing viscosity of the brine finally causes the diffusion coefficient to decrease. Figure 4 shows that these same effects are mirrored in T_1.

The quadrupolar spin-lattice relaxation appears to be so effective in the bulk phase that ^{23}Na T_1 measurements in cores are only slightly smaller than those in bulk brine with little additional contribution from surface relaxation. Table 4 compares the bulk 4.0 M NaCl brine T_1 with T_1's measured on a suite of carbonates and sandstones saturated with this brine.

1-D DIFFUSION EXPERIMENTS

In this section we describe one-dimensional sodium NMR diffusion measurements. Figure 5 shows the simple apparatus. The 2-in. OD by 1-in. long cylindrical cores are epoxied on the circumference and one face to prevent bulk flow and limit diffusion to a one-dimensional geometry. The large 2-in. OD x 4-in. long brine chamber at the open face keeps the boundary condition at nearly constant concentration. The cores are initially saturated with 0.432 M KCl brine under vacuum. Just before starting the measurements the chamber is filled with NaCl brine of the same density as the KCl solution (0.5 M NaCl, density = 1.0203 g/cm^3). The core is then placed horizontally in the NMR spectrometer and the entire cell

surrounded by styrofoam to reduce thermal gradients. Convective flow is eliminated because the two brine solutions have identical densities and virtually identical osmotic pressures.

As shown in Figure 4, the diffusion coefficient of Na^+ is concentration dependent, particularly above 1M NaCl. A brine concentration below 1M NaCl should therefore be utilized in order to obtain the most accurate values of diffusion coefficient: below 1 M NaCl the sodium diffusion coefficient is nearly constant (1.334×10^{-5} cm^2/sec within ±2% from 0 M to 0.9 M NaCl). Moreover, in this concentration range the Na^+ diffusion coefficient in NaCl brine is virtually identical to the Na^+ diffusion coefficient in KCl brine.[6] This enables the concentration profiles to be matched with a single value for the sodium diffusion coefficient.

One-dimensional profiles of ^{23}Na concentration were obtained every twenty minutes down the axis of the sample as the sodium diffused into the core. Table 5 lists the NMR acquisition parameters. The NMR signal is averaged over the core cross section (X,Y) and profiled along the horizontal core axis (Z) using a magnetic field gradient readout in the Z direction.

Figure 6 shows ^{23}Na concentration profiles over four days of sodium diffusion into a Berea sandstone with a porosity of 22.94%. Assuming the diffusion coefficient is constant, there is no convection, and that diffusion occurs only in the axial direction of the core, the solution of the diffusion equation for 1-D diffusion to a barrier is

$$C(z,t) = C_o \sum_{n=0}^{\infty} (-1)^n \left\{ \operatorname{erfc}\left[\frac{(2n+1)\ell - z}{2\sqrt{Dt}}\right] + \operatorname{erfc}\left[\frac{(2n+1)\ell + z}{2\sqrt{Dt}}\right] \right\} \quad (1)$$

Here C(z,t) is the sodium concentration at distance (z) and time (t), C_o is the concentration at the open face, z is the distance from the closed face, ℓ is the thickness of the core, and D is the effective diffusion coefficient. The numerical fit in Figure 6 results in an effective diffusion coefficient of 0.58×10^{-5} cm^2/sec for the Berea sandstone. Using a bulk sodium diffusion coefficient D_o of 1.334×10^{-5} cm^2/sec, the tortuosity of the Bentheim core is

$$T = \sqrt{D_o/D} = 1.52 \quad (2)$$

The tortuosity, in turn, is related to formation factor F and porosity ϕ by

$$T^2 = F \cdot \phi \ , \quad (3)$$

from which the diffusional formation factor is 10.0. This is smaller than the electrical formation factor $\frac{1}{\phi^{1.78}} = 13.7$.

SODIUM IMAGING

In this section, we report on the implementation of ^{23}Na NMR imaging techniques. One goal of ^{23}Na imaging is to visualize filtrate invasion in cores without the use of dopants in the drilling mud. This assumes, as is usually the case, that the sodium concentration of the drilling mud differs from that in the formation brine. Visualizing filtrate invasion by ^{23}Na NMR is complementary to X-ray CT imaging of the invasion process because CT responds primarily to the barite solids in the drilling mud.

As an example of ^{23}Na imaging, the transport of brines into and out of Berea and Bentheim sandstone cores was imaged. Table 6 shows the ^{23}Na imaging parameters. Compared to ^{1}H imaging of cores, the minimum update time in the imaging sequences was reduced from 1000 msec to 100 msec because of the inherently short T_1 of ^{23}Na. This reduction in update times greatly improves the signal-to-noise for ^{23}Na imaging.

The sandstone cores were 2-in. OD by 4-in. long and initially saturated with 250,000 ppm brine. The cores were allowed to soak for various periods of time in fresh water. After each soak time, the core was removed, surface-dried and NMR-imaged in the same orientation. The NMR image is a 1-in. thick slice-selective image at the center of the core, where the movement of salt should be predominantly radial. The difference in brine densities is sufficiently great that the brine transport occurs predominantly by convection.

Figure 7a depicts the transport of ^{23}Na out of the Berea core with increased exposure to fresh water. The radial effusion of ^{23}Na is surprisingly nonuniform. In order to check the reversibility of the experiment, following exposure to fresh water, the core was allowed to soak in 250,000 ppm brine for various periods of time in order to visualize the infusion of NaCl back into the core (Figure 7b). The same nonuniform radial pattern is found for the reverse transport process.

The advantage of ^{23}Na over ^{1}H for imaging salinity variations is clearly depicted in Figure 8a which shows ^{23}Na and ^{1}H images of this Berea core after 256 minutes of soaking in the 250,000 ppm brine. Whereas the ^{1}H density image is fairly uniform over the core, the corresponding ^{23}Na image shows a pronounced nonuniform brine distribution due to nonuniform sodium transport into the core. The ^{1}H density image does show the effect of high sodium concentration, however; the regions of reduced proton density (light blue and yellow) in the ^{1}H image match the high salinity (red) region in the ^{23}Na image. This is because the proton density of water is reduced 10% by the high salt content.

Similar brine transport experiments were carried out on the Bentheim core initially saturated with 250,000 ppm brine and exposed to fresh water for up to several hours, as shown in Figure 8b. As in the case of the Berea core, the transport is again nonuniform, with the upper portion of the core experiencing a higher rate of transport than the lower portion. The higher rate of transport is correlated with the higher porosity, and presumably higher permeability, in the upper portion of the core (see image 8b at t=0).

CONCLUSIONS

^{23}Na NMR offers an exciting approach to the measurement and visualization of brine salinities in cores. Although ^{23}Na has low sensitivity, ^{23}Na NMR imaging is practical because of the short spin-lattice relaxation times due to quadrupolar interactions. Accurate sodium concentrations can be obtained easily in clay-free carbonates, and sodium diffusion and sodium filtrate invasion can be imaged. The potential applicability in shaly sands and shales must still be studied.

ACKNOWLEDGMENTS

We gratefully acknowledge the help of Larry J. Bielamowicz in preparing the core samples. We also acknowledge very useful discussions with George L. Stegemeier of Shell Development Co. and with William Edelstein of General Electric Co.

TABLE 1

NMR SENSITIVITIES OF COMMON NUCLEI

Nuclei	Spin	Gamma (MHz/Kgauss)	Natural Abundance (%)	Sensitivity Relative	Sensitivity Absolute
^{1}H	1/2	4.2575	99.98	1.0	1.0
^{2}H	1	0.6535	0.015	9.65×10^{-3}	1.45×10^{-6}
^{13}C	1/2	1.0705	1.108	1.59×10^{-2}	1.76×10^{-4}
^{19}F	1/2	4.0053	100.0	0.83	0.83
^{23}Na	3/2	1.1262	100.0	9.25×10^{-2}	9.25×10^{-2}

TABLE 2

^{23}Na NMR LINEWIDTHS (FWHM) FOR SEVERAL MINERALS AT 200 MHz

Mineral	Linewidth (Hz)
167,000 ppm NaCl brine in Indiana limestone	250
Crystalline NaCl	2,780
Sodium Carbonate	5,660
Sodium Metasilicate	4,000
Sodium Bentonite (dry)	11,350
Sodium Bentonite (hydrated, distilled water)	950

TABLE 3

^{23}Na NMR vs WEIGHT OF SODIUM FOR VARIOUS LITHOLOGIES

Rock	^{23}Na NMR (g)	Weight Sodium (g)	Error %
Indiana limestone	0.256	0.253	1.19
Austin limestone	0.422	0.419	0.72
Bakers dolomite	0.256	0.254	0.79
San Andres dolomite	0.293	0.277	5.78
Bentheim sandstone	0.400	0.416	-3.85
Berea sandstone	0.363	0.388	-6.44

TABLE 4

^{23}Na SPIN-LATTICE RELAXATION TIMES FOR VARIOUS LITHOLOGIES

Rock	^{23}Na T_1 (ms)
4.0 M NaCl	42.0 ± 0.2
Indiana limestone	32.4 ± 0.3
Austin limestone	33.2 ± 0.3
Bakers dolomite	32.8 ± 0.2
San Andres dolomite	35.1 ± 0.3
Bentheim sandstone	39.5 ± 0.2
Berea sandstone	37.5 ± 0.3

TABLE 5

^{23}Na PROFILING PARAMETERS

Recycle Time:	200 ms
180 degree pulse length:	114 microseconds
Field of View:	168 mm
Read Out Gradient:	850 Hz/mm
Echo Time:	2.5 ms
Number of Averages:	1280
Total Profiing Time:	6 minutes

TABLE 6

^{23}Na IMAGING PARAMETERS

Recycle Time:	100 ms
Slice Thickness:	25 mm
Image Resolution:	256 x 256
Field of View:	120 mm x 120 mm
Read Out Gradient:	1200 Hz/mm
Echo Time:	3 ms
Number of Averages:	64
Total Imaging Time:	28 minutes

REFERENCES

1. Timur, A. (1969), "Pulsed nuclear magnetic resonance studies of porosity, movable fluid and permeability of sandstones," J. Pet. Tech., V. 246, pp. 775–786.

2. Tutunjian, P. N. and Vinegar, H. J. (1990), "Petrophysical applications of automated proton high resolution NMR spectroscopy," SCA 4th Annual Technical Conference Paper SCA-9020, Dallas, August 14–16.

3. Vinegar, H. J., Tutunjian, P. N., Crabtree, P. T., Raffaldi, F. J., DiFoggio, R., and Edelstein, W. A. (1989), "NMR spectroscopy of tight, gypsum-bearing carbonates," paper HH, 30th Annual SPWLA Symposium, Denver, June 11–14.

4. Edelstein, W. A., Vinegar, H. J., Tutunjian, P. N., Roemer, P. B., and Mueller, O. M. (1988), "NMR imaging for core analysis," paper 18272, 63rd Annual Technical Conference of the SPE, Houston, October 2–5, pp. 101–112.

5. Vinegar, H. J., Tutunjian, P. N., Edelstein, W. A., and Roemer, P. B. (1991), "Whole-Core Analysis by ^{13}C NMR," in SPE Formation Evaluation, Vol. 6, No. 2, June, 1991, pp. 183–189.

6. Vinegar, H. J., Tutunjian, P. N., Edelstein, W. A., and Roemer, P. B. (1989), "Determining carbonate content of cores by ^{13}C NMR," 1989 SCA Conference Paper 8901, New Orleans, August 2–3.

7. Wang, J. H. (1954), "Effect of ions on the self–diffusion and structure of water in aqueous electrolytic solutions," J. Phys. Chem., Vol. 58, pp. 686–692.

8. Abragam, A. (1961), "Principles of Nuclear Magnetism," Oxford University Press, London, pp. 313–348.

FIG 1A. 23Na NMR INTENSITY vs CONC. NACL BRINES AT 25 C (HIGH SALINITY)

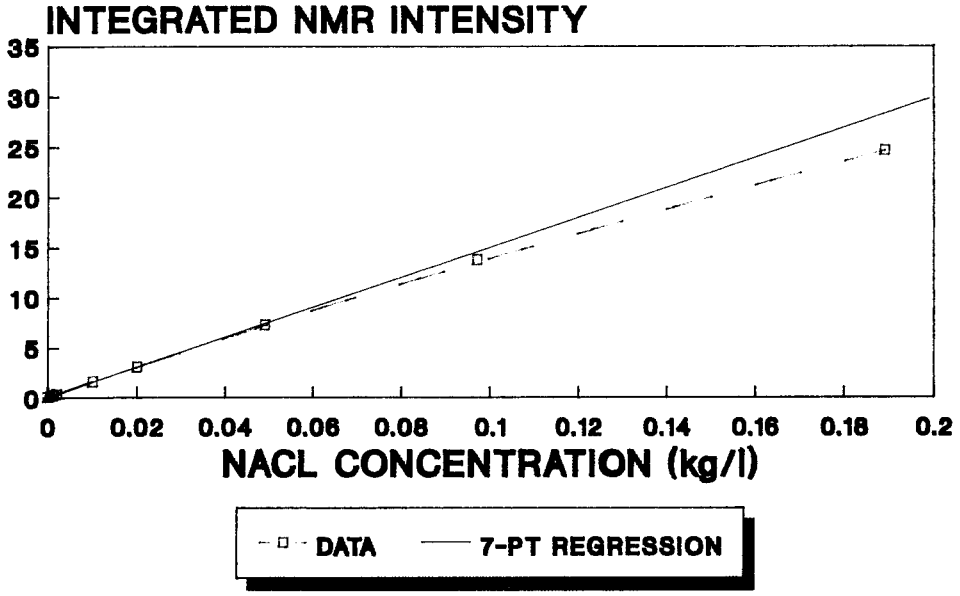

FIG 1B. 23Na NMR INTENSITY vs CONC. NACL BRINES AT 25 C (LOW SALINITY)

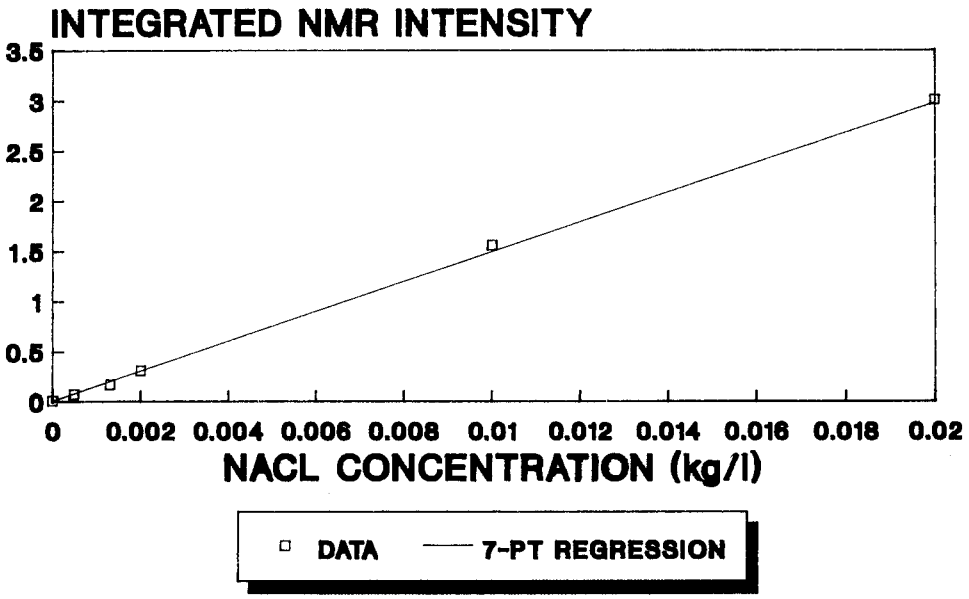

FIG 2A. 23Na NMR INTENSITY vs CONC. INDIANA LIMESTONE (HIGH SALINITY)

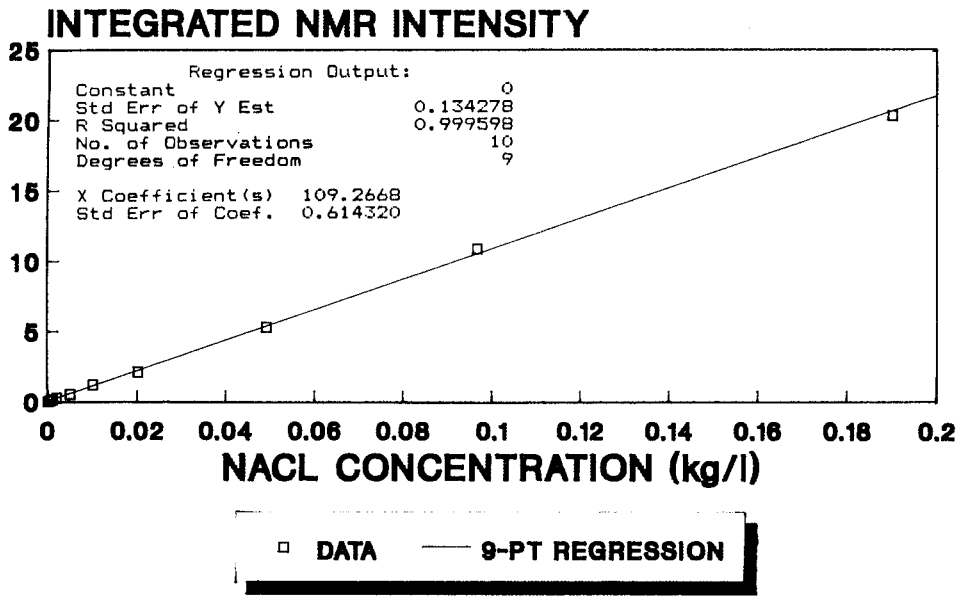

FIG 2B. 23Na NMR INTENSITY vs CONC. INDIANA LIMESTONE (LOW SALINITY)

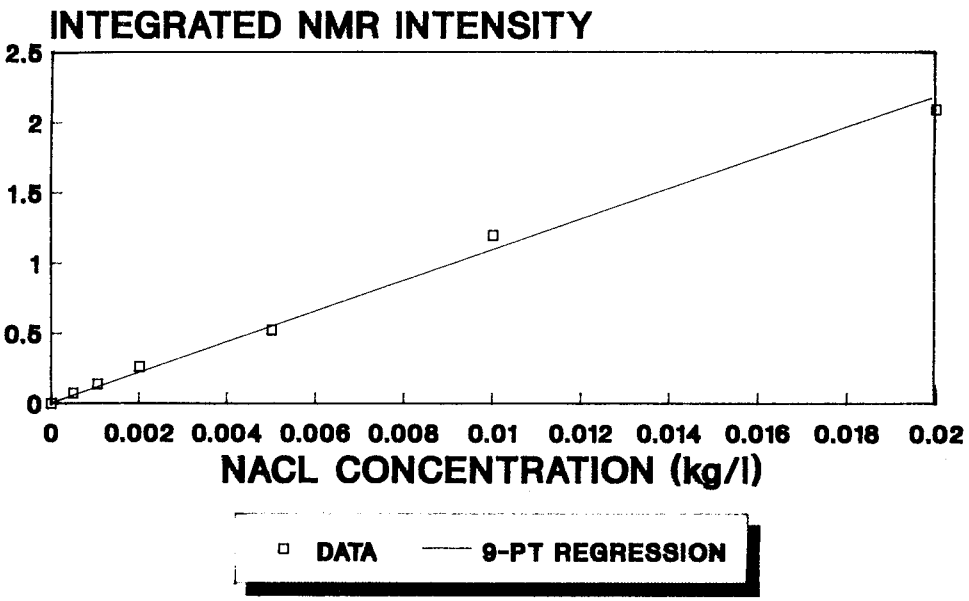

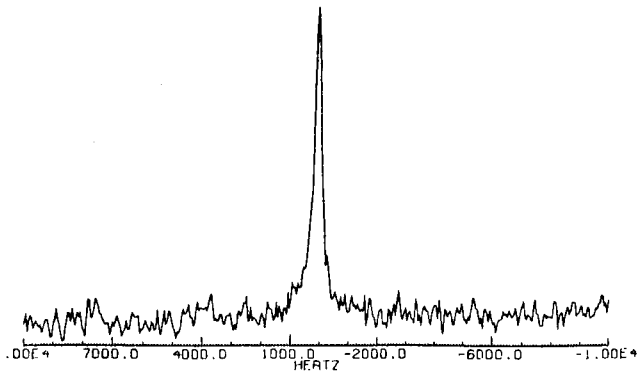

a) 200,000 ppm NaCl brine in Indiana Limestone

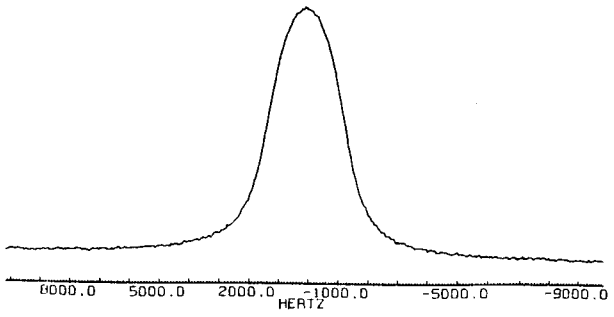

b) Crystalline Sodium Chloride

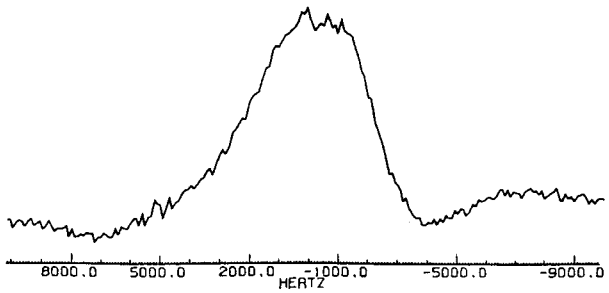

c) Sodium Carbonate

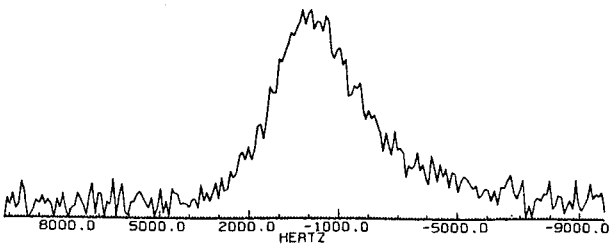

d) Sodium Metasilicate

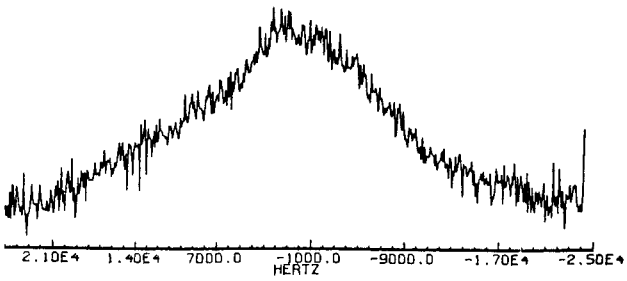

e) Dry Sodium Bentonite

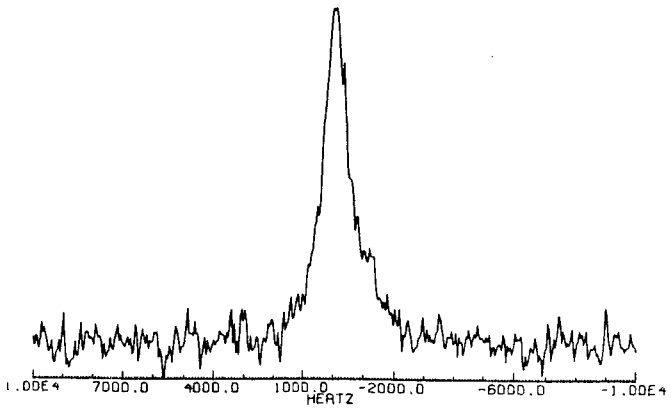

f) Sodium Bentonite hydrated with distilled water

Fig. 3 ^{23}Na NMR SPECTRA OF SODIUM-BEARING MINERALS

FIG 4. 23Na NMR T1 and DIFFUSION COEFF. vs SQRT (CONC) for NACL BRINES

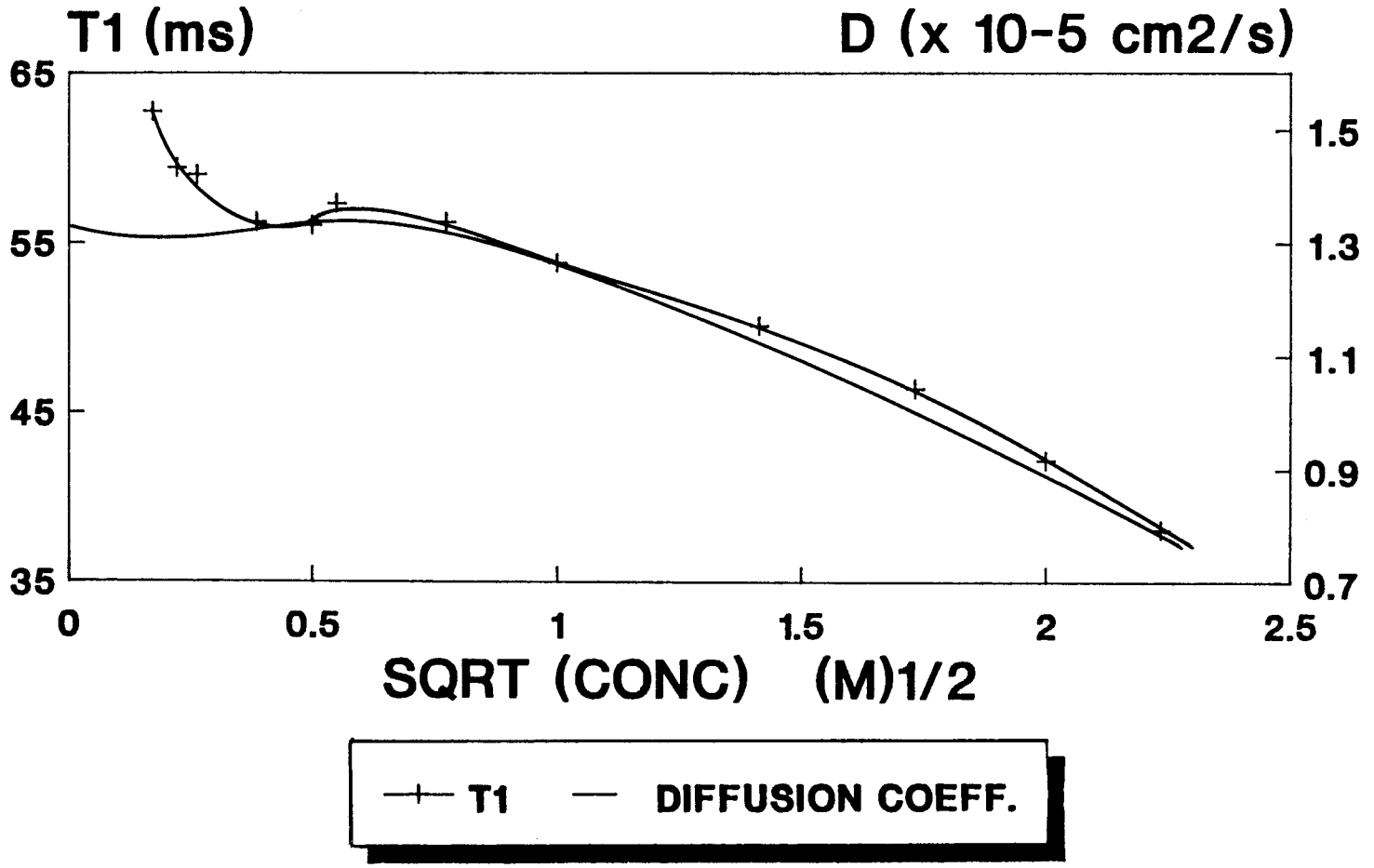

T = 25°C

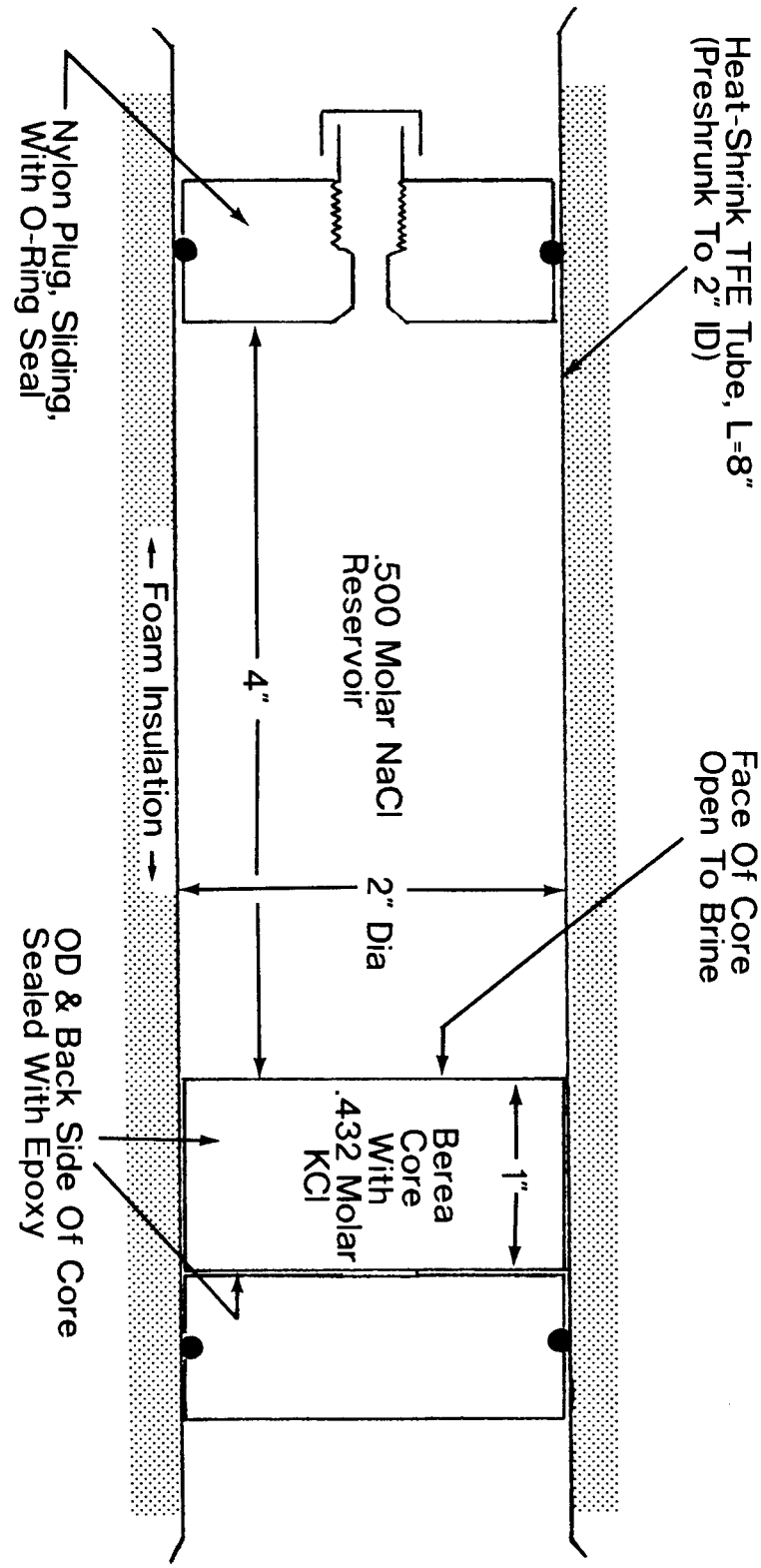

Fig. 5 CROSSECTION OF APPARATUS FOR 1-D ^{23}Na DIFFUSION PROFILING EXPERIMENTS

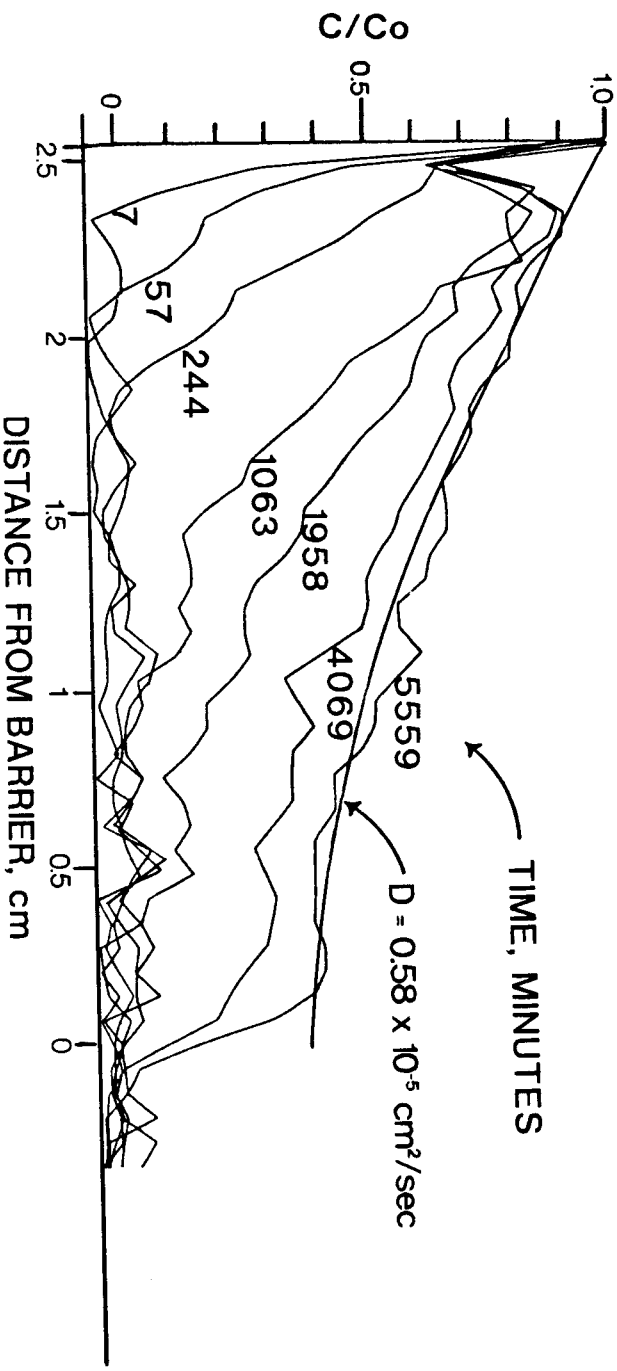

Fig. 6 ^{23}Na CONCENTRATION PROFILES VS. TIME IN BEREA SANDSTONE

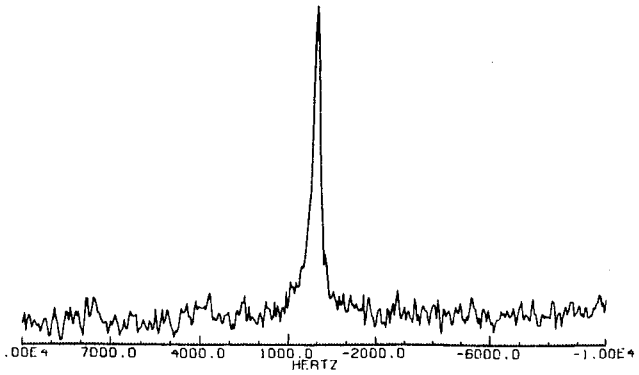

a) 200,000 ppm NaCl brine in Indiana Limestone

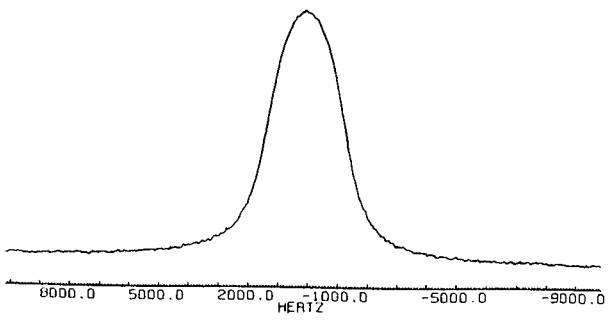

b) Crystalline Sodium Chloride

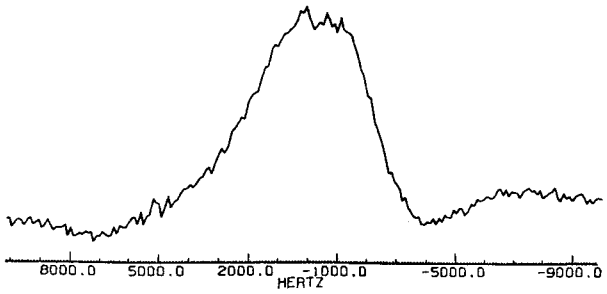

c) Sodium Carbonate

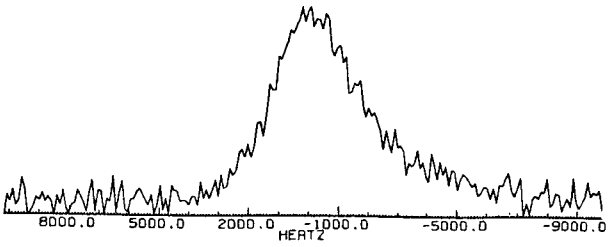

d) Sodium Metasilicate

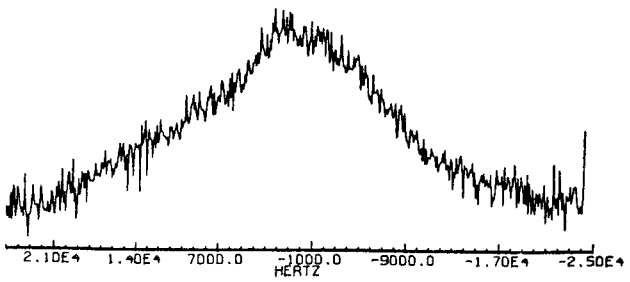

e) Dry Sodium Bentonite

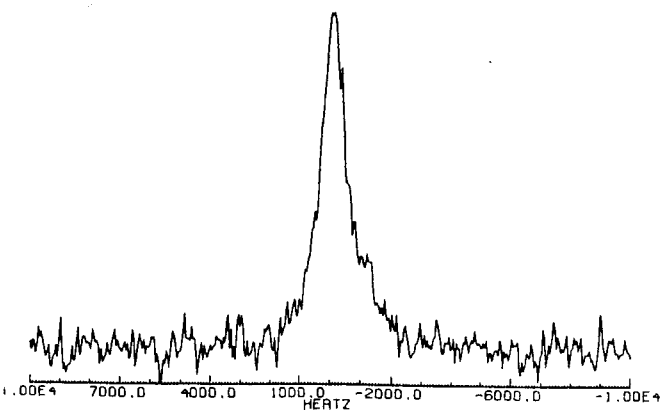

f) Sodium Bentonite hydrated with distilled water

Fig. 3 ^{23}Na NMR SPECTRA OF SODIUM-BEARING MINERALS

FIG 4. 23Na NMR T1 and DIFFUSION COEFF. vs SQRT (CONC) for NACL BRINES

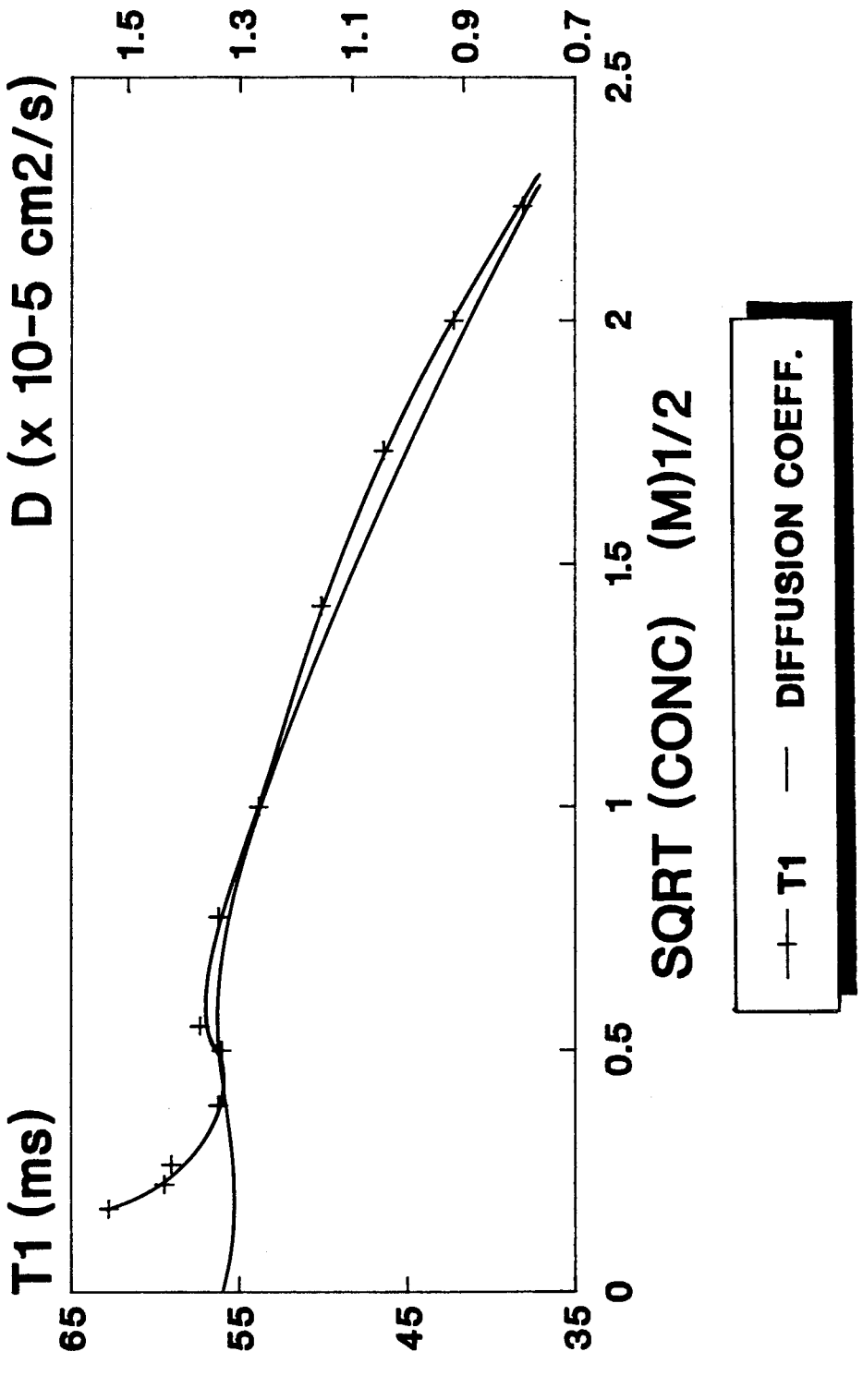

T = 25°C

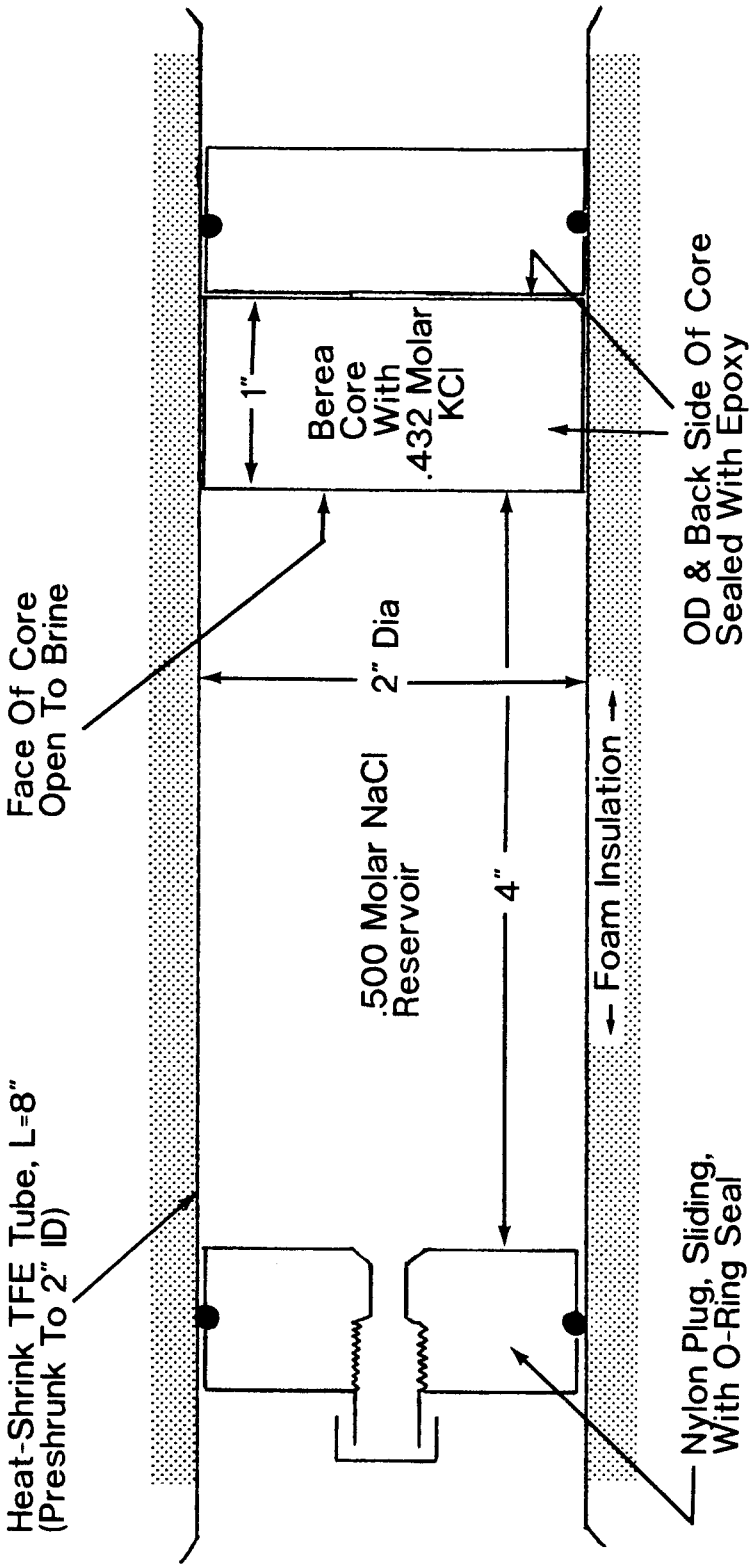

Fig. 5 CROSSECTION OF APPARATUS FOR 1-D ^{23}Na DIFFUSION PROFILING EXPERIMENTS

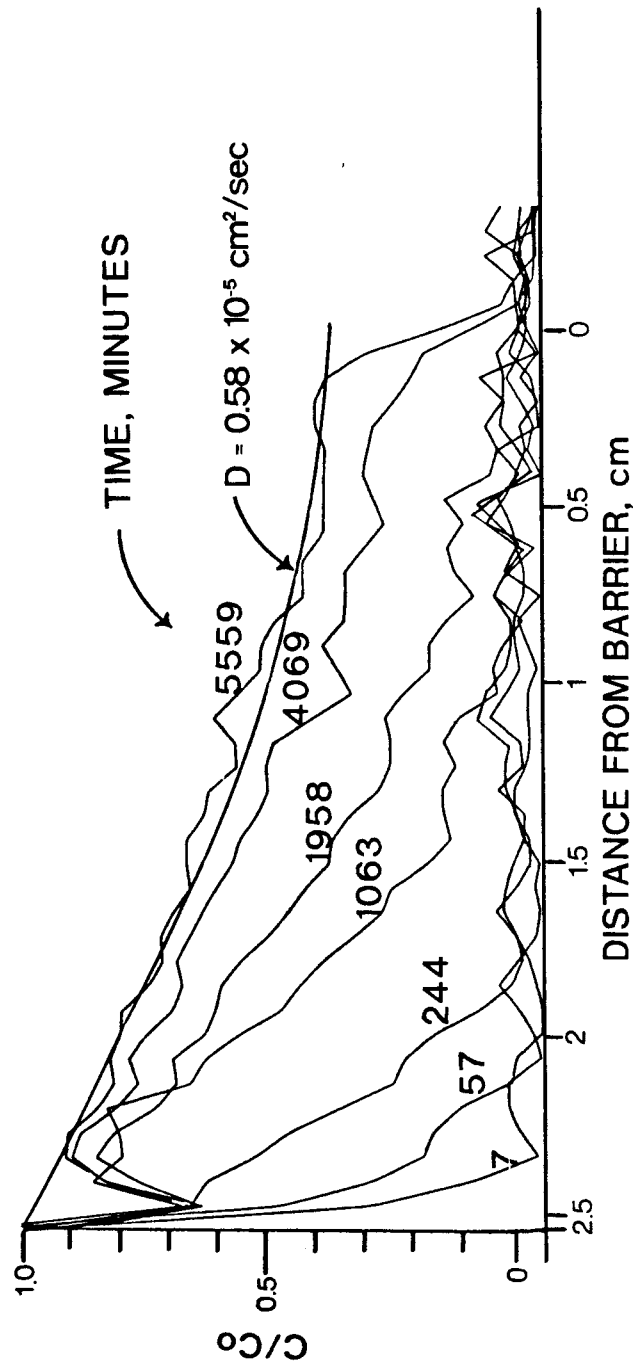

Fig. 6 ^{23}Na CONCENTRATION PROFILES VS. TIME IN BEREA SANDSTONE

Fig. 7a Effusion of ^{23}Na from 250,000 ppm NaCl-Saturated Berea Sandstone

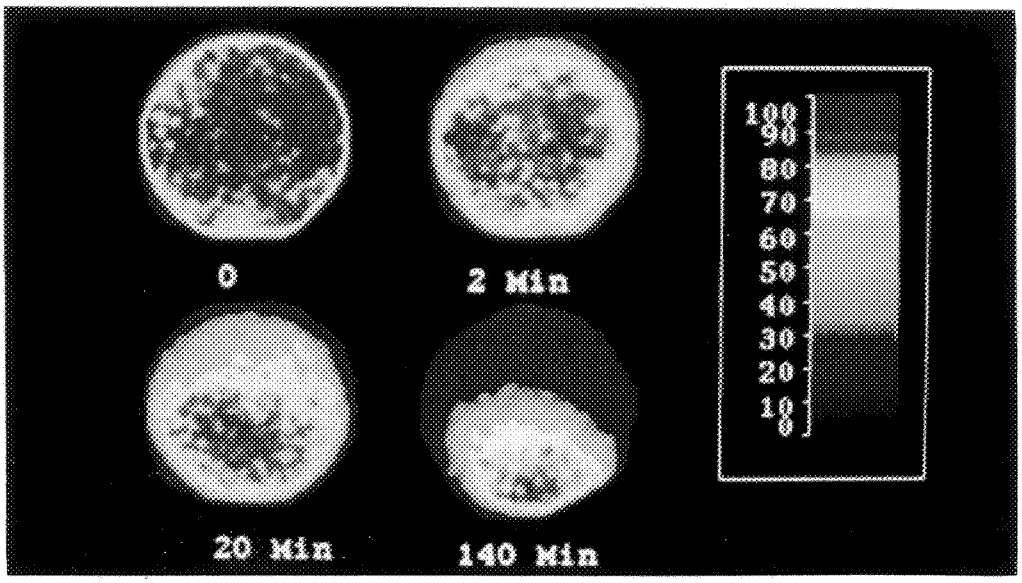

Fig. 7b Infusion of 250,000 ppm ^{23}Na into Fresh Water-Saturated Berea Sandstone

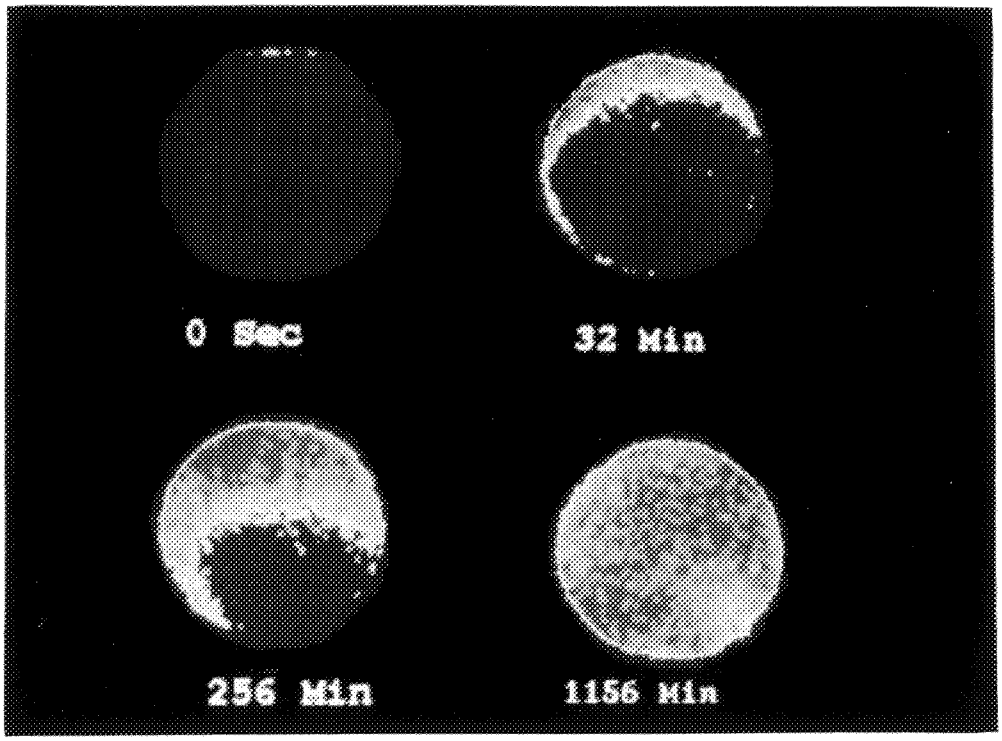

Fig. 8a ^{23}Na and ^{1}H NMR Images of Berea Sandstone Soaked in 250,000 ppm NaCl

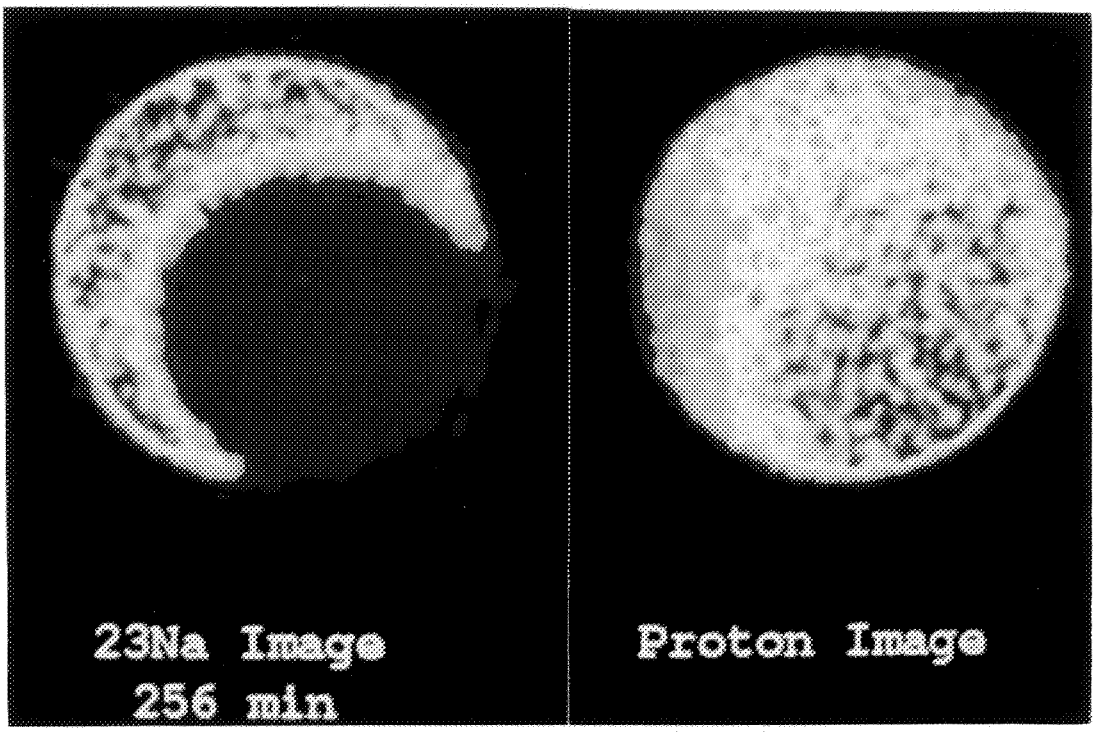

Fig. 8b Effusion of ^{23}Na from 250,000 ppm NaCl-Saturated Bentheim Sandstone